THE JOURNAL OF PHYSICAL CHEMISTRY B

pubs.acs.org/JPCB Article

Molecular Model for the Surface-Catalyzed Protein Self-Assembly

Yangang Pan, Siddhartha Banerjee, Karen Zagorski, Luda S. Shlyakhtenko, Anatoly B. Kolomeisky,* and Yuri L. Lyubchenko*

Cite This: J. Phys. Chem. B 2020, 124, 366−372 Read Online

ACCESS | Metrics & More | Article Recommendations | Supporting Information

ABSTRACT: The importance of cell surfaces in the self-assembly of proteins is widely accepted. One biologically significant event is the assembly of amyloidogenic proteins into aggregates, which leads to neurodegenerative disorders like Alzheimer's and Parkinson's diseases. The interaction of amyloidogenic proteins with cellular membranes appears to dramatically facilitate the aggregation process. Recent findings indicate that, in the presence of surfaces, aggregation occurs at physiologically low concentrations, suggesting that interaction with surfaces plays a critical role in the disease-prone aggregation process. However, the molecular mechanisms behind the on-surface aggregation process remain unclear. Here, we provide a theoretical model that offers a molecular explanation. According to this model, monomers transiently immobilized to surfaces increase the local monomer protein concentration and thus work as nuclei to dramatically accelerate the entire aggregation process. This physical−chemical theory was verified by experimental studies, using mica surfaces, to examine the aggregation kinetics of amyloidogenic α-synuclein protein and non-amyloidogenic cytosine deaminase APOBEC3G.

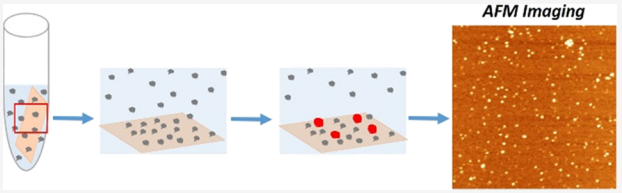

INTRODUCTION

The assembly of proteins into aggregates of various types is a general phenomenon found frequently in both natural and industrial processes.[1,2] Different types of protein aggregates are commonly observed. For example, proteins can self-assemble into filamentous aggregates; the actin filament is one of the numerous examples of this process. Another, and the most known, example is the formation of aggregates by amyloidogenic proteins. According to the current views, the formation of amyloidogenic aggregates is a hallmark in the development of numerous disorders, including neurodegenerative diseases such as Alzheimer's disease.[3] Although the self-assembly of protein aggregates can take place in solution, the importance of membrane surfaces in such processes is also acknowledged (e.g., refs 4−6).

In general, the aggregation process is accelerated in the presence of membranes (e.g., ref 7 and the references therein). With respect to Alzheimer's disease, great interest has been given to the role of membranes in disease pathogenesis and in facilitating the assembly of amyloid fibrils (e.g., reviews in refs 6 and 8−12). Importantly, the inclusion of cholesterol and gangliosides into membranes changes the structure and stability of amyloid aggregates; these changes appear to contribute to the neurotoxic effect of aggregates.[10,11] However, a molecular mechanism explaining the role of membrane surfaces toward protein aggregation and related chemical processes remains poorly understood.

Recent studies have shown that, similar to membranes, surfaces such as glass,[13] mica,[14,15] and zeolites[16] also accelerate the aggregation process for various amyloidogenic proteins. Importantly, amyloid aggregates, primarily fibrils, have been imaged using electron microscopy[16] and AFM.[14,15] As such, the use of solid surfaces has made it possible to partially visualize the molecular mechanism behind the surface-acceleration effect. According to the model proposed elsewhere,[14,15] the accelerated aggregation is due to the fast, two-dimensional diffusion of amyloid peptide molecules at the surface−liquid interface.

AFM has been used to directly observe the accelerated aggregation of amyloid peptides and the α-synuclein (α-Syn) protein on mica surfaces. Results demonstrated that the assembly of proteins into aggregates took place at low protein concentrations, while no aggregation was detected in the bulk solution.[17] Importantly, time-lapse AFM experiments in liquid did not reveal fast mobility of molecules at the mica−liquid interface.[17] These data were also in line with observations performed using time-lapse high-speed AFM.[18,19] These results suggest that an alternative chemical mechanism of accelerated aggregation on the surface that does not include surface diffusion must be realized. Such a mechanism is proposed in the current work.

Here, a novel theoretical model is provided to explain the molecular mechanism of the surface-mediated catalysis behind the protein aggregation process. According to this model,

Received: October 25, 2019
Revised: December 17, 2019
Published: December 22, 2019

https://dx.doi.org/10.1021/acs.jpcb.9b10052
J. Phys. Chem. B 2020, 124, 366−372

aggregation starts with protein monomers transiently attaching to the surface due to nonspecific chemical interactions. This process increases the local concentration of proteins, which in turn increases the probability of oligomerization reactions to occur on the surface. Based on this model, aggregation occurs by the assembly of oligomers on these transiently bound monomers. This theoretical prediction was experimentally tested using two proteins that follow different aggregation pathways. One such protein, α-Syn, is a typical amyloidogenic protein capable of assembling into aggregates of various morphologies, including fibrils. The other protein, cytosine deaminase APOBEC3G (A3G), assembles into oligomers of various sizes depending on the protein concentration (e.g., ref 20 and the references therein).

MATERIALS AND METHODS

α-Synuclein Sample Preparation. Monomers of α-Syn (A140C, where the C-terminal alanine was replaced by cysteine) were freshly prepared as previously described.[21] In brief, 0.4−0.8 mg of lyophilized powder was dissolved in 200 μL of water (pH 11.0; adjusted with 1 M NaOH solution). Then 1 μL of 1 M dithiothreitol (DTT) was added to break the disulfide bonds. Next, 300 μL of 10 mM sodium phosphate buffer (pH 7.0) was added and mixed thoroughly. The obtained mixture of solution was filtered through Amicon filters with a molecular weight cutoff of 3 kDa and vortexed at 14000 rpm for 15 min. This process was repeated three times to remove the DTT from the solution. The concentration of the α-Syn stock was measured by spectrophotometry (Nanodrop ND-1000) using molar extinction coefficients of 1280 and 120 $cm^{-1}\cdot M^{-1}$ for tyrosine and cysteine, respectively, at 280 nm. All samples were prepared with the use of functionalized 1-(3-aminopropyl)silatrane (APS)−mica as previously described.[22−24] APS−mica surfaces were prepared by incubating freshly cleaved mica surfaces in 167 μM APS solution for 30 min, then rinsed thoroughly with Millipore water, and dried with argon flow. Small pieces of the APS−mica surface were incubated in solutions of 10 or 2 nM α-Syn in low-protein-binding Eppendorf tubes. The substrates were removed from the tubes at the desired time points, rinsed with Millipore water, dried with argon flow, and imaged in tapping mode at ambient conditions. A tube containing the same protein solution (10 or 2 nM) was kept incubated at room temperature, and 5 μL of solution was taken out at similar time points and deposited onto APS−mica surfaces to compare the aggregation in bulk solution.

A3G Sample Preparation. For the on-surface aggregation experiments, several Eppendorf tubes with 1 or 2 nM A3G (800 μL) solution in binding buffer (containing 50 mM HEPES (pH 7.5), 100 mM NaCl, 5 mM $MgCl_2$, and 1 mM DTT) were prepared, which according to the previous data[20] correspond to the monomeric state of A3G. A piece of APS-modified mica was immersed into each Eppendorf tube, as shown schematically in Figure 1. After 2 min, a piece of mica was removed from the tube, rinsed with deionized water, and dried with argon gas. The same procedure was followed for 15 min, 30 min, 60 min, 120 min, 5 h, and 18 h of incubation time. For control experiments, A3G solutions were kept in a separate tube without the mica piece. For each incubation time, as used for on-surface experiments, 10 μL of A3G solution was deposited onto advance prepared APS−mica surfaces for 2 min, washed with deionized water, and dried with Ar for AFM imaging. The justification for the use of 2 min of deposition time is presented in Figure S7. A similar procedure was performed for on-surface aggregation of 1 nM A3G with the use of a freshly cleaved bare mica surface.

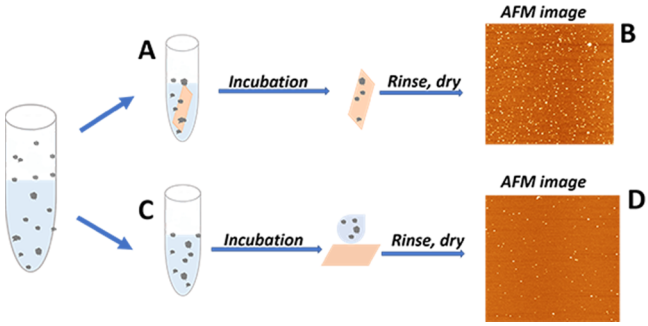

Figure 1. Schematic presentation of the experimental setup to monitor (A) the on-surface A3G aggregation and, in parallel, (C) control experiments for aggregation in bulk solution. Panels (B) and (D) are AFM images of on-surface and bulk aggregation, respectively.

PriA Sample Preparation. For on-surface aggregation experiments with the PriA protein, we used the same procedure as A3G protein.

AFM Imaging and Analysis. Images were acquired in tapping mode in air with a Multimode Nanoscope III system (Bruker-Nano; Santa Barbara, CA) using TESPA probes with a spring constant of 42 N/m at resonance frequencies of 310−340 Hz.

The volume of protein was obtained using the Enum feature tool of FemtoScan online software (Advance Technologies Center, Moscow, Russia); the measurements were made based on cross section values as previously described in detail.[25] Briefly, the volume of the protein was calculated from the measurements of the height and diameter of each protein molecule on the AFM image. For each time interval, several AFM images with more than 300 protein molecules were analyzed, and the volume values were measured. For the initial time point, when both A3G and α-Syn are monomers, the data were assembled into a histogram (Figure S11) and fitted with a Gaussian. The maximum in the Gaussian distribution was assigned to the volume of the monomeric protein based on the molecular weight value for monomers of α-Syn (~14 kDa) and A3G (~49 kDa) and the conversion coefficient, as described elsewhere.[26] For the A3G monomer (Figure S11A) and α-Syn monomer (Figure S11B), the volumes are 66 and 26 nm^3, respectively. The standard deviation, obtained from the Gaussian distribution, was used as a parameter for the separation of the monomers from oligomers. So, for the A3G protein, the numbers of protein molecules with volumes in the range of 66 ± 19 nm^3 and for α-Syn in the range of 26 ± 6 nm^3 were considered monomers. The numbers of protein molecules with volumes larger than 85 and 32 nm^3 for A3G and α-Syn, respectively, were counted as oligomers. The ratio of the number of oligomers to the number of monomers over time was plotted on a graph.

RESULTS AND DISCUSSION

Theoretical Model for the Surface-Mediated Protein Aggregation. To explain the complex processes of surface-assisted protein aggregation, a new theoretical model was further developed. The main assumptions for this theoretical model are as follows:

https://dx.doi.org/10.1021/acs.jpcb.9b10052
J. Phys. Chem. B 2020, 124, 366−372

(1) Due to intrinsic chemical interactions with surfaces, protein monomers very quickly bind to the surface and establish an effective equilibrium between surface-bound and free monomers in solution. The equilibrium coverage is given by the parameter $0 < \theta < 1$, which describes what fraction of the surface is covered by protein monomers.

(2) The effective concentration of monomers near the surface increases in comparison to concentration in bulk solution, and this accelerates the rates of oligomerization on the surface.

(3) The formation of oligomers is an effectively irreversible process due to strong bonds between monomers in them.

To examine these arguments quantitatively, $C(t)$ can be defined as the time-dependent concentration of protein monomers in solution. At $t = 0$, $C(t) = C_0$. This represents the initial concentration of proteins in solution. Assuming that the surface area is equal to L^2 and the molecular volume of one protein monomer is $v_0 \sim d^3$, the maximum possible number of monomers on the surface can be estimated as follows:

$$N_{max} = \frac{L^2}{d^2} \tag{1}$$

The number of adsorbed proteins can be given by N_1:

$$N_1 = \theta N_{max} \tag{2}$$

For a solution in the absence of a surface, as shown in detail in the Supporting Information, the reaction rate for the formation of all oligomers can be calculated as follows, where k is the bulk rate constant:

$$R_0 = kC^2 \tag{3}$$

This expression assumes that the reaction of dimerization is bimolecular because it requires two monomers to react, leading to quadratic dependence of the reaction rate. The formation rates of larger oligomers cancel each other as explained in the Supporting Information, leaving only the rate of production of dimers. However, in the presence of the surface, the following equation can be applied:

$$R_1 = kC^2 + k_sCC_1 \tag{4}$$

In the equation above, k_s represents the reaction rate for the formation of dimers on the surface, and C_1 represents the concentration of the protein monomers in the volume immediately surrounding the surface. This equation can be understood in the following way. The first term describes the reaction in the bulk (as in eq 3), while the second term describes the reaction that takes place on the surface. This term should be proportional to the product of concertation of free monomers in solution C and the monomers absorbed on surface C_1. We assume that the chemical reaction is taking place via collisions of free monomers with the absorbed monomers on the surface.

The concentration in the volume immediately surrounding the surface can be estimated using eqs 1 and 2, with N_A being Avogadro's number:

$$C_1 = \frac{N_1}{N_A L^2 d} = \frac{\theta N_{max}}{N_A L^2 d} = \frac{\theta}{N_A v_0} \tag{5}$$

In these calculations, we assume that the volume around the surface is equal to L^2d. There is some arbitrariness in choosing this volume. For example, we can take, instead of one monomer diameter's d, several d, and this would slightly modify the numbers. However, importantly, the main prediction of our theoretical approach will not change because it is based on the idea that the concentration of protein monomers near the surface is increased in comparison with bulk values.

Now, the acceleration factor in the reaction rate due to the presence of the surface at earlier times can be evaluated:

$$\gamma = \frac{R_1}{R_0} = 1 + \frac{k_s}{k}\frac{C_1}{C_0} \approx \frac{k_s}{k}\frac{C_1}{C_0} = \frac{k_s}{k}\frac{\theta}{C_0 N_A v_0} \tag{6}$$

To estimate this factor using more or less realistic parameters, very low coverage is assumed, with $\theta = 0.001$ (0.1%), $C_0 = 1$ nM (as used in our experiments), and $v_0 \sim 100$ nm^3. The ratio $\frac{k_s}{k}$ is equal to 0.1, and this is because the reaction rate constant, which is the reaction rate per unit concentration of reagents, on the surface is expected to be smaller than that in bulk solution due to steric constraints, slower collision speeds, and possible conformational changes. Note that the steric effect here is associated with the surface geometrically restricting the access to some parts of the bound protein and lowering the number of collisions that could lead to the successful chemical reaction. In addition, the molecules on the surface do not move, and this decreases the relative molecular collisional speeds, lowering the reaction rate. Conformational changes might also complicate the formation of protein−protein bonds. It is hard to quantitatively describe all these effects, but we can reasonably assume that the rate constant on the surface at least is 1 order of magnitude slower than that in the bulk. This is what was used in the estimation of $k_s/k = 0.1$. Finally, our calculations produce $\gamma \sim 1.6 \times 10^3$, which represents a markedly accelerated aggregation process due to the presence of the surface.

These calculations show that the aggregation in bulk solution is relatively slow; the dominating chemical process in the system is the formation of dimers on the surface.

We generalized the theory described for the dimer formation to a more realistic situation: when oligomers of various sizes are assembled. This can be described by the following overall quasi-chemical reaction, where C represents bulk protein monomers, C_1 represents surface-bound protein monomers, and C_{oligo} represents surface-bound oligomers of all sizes, that is, the combined concentration of dimers, trimers, and so on (see the Supporting Information for more explanations):

$$C + C_1 \rightarrow C_{oligo} \tag{7}$$

Note that our main object of consideration is the surface and the protein oligomerization processes that are taking place there.

Next, $C_{oligo}(t)$ can be given as the time-dependent concentration of all oligomers, with $C_{oligo}(t = 0) = 0$ and the rate constant k_s. As such, neglecting reactions in the bulk as we argued above, the chemical kinetic equations for this system can be written as follows (see the Supporting Information for more details):

$$\frac{dC(t)}{dt} = -k_sC_1C(t) \tag{8}$$

https://dx.doi.org/10.1021/acs.jpcb.9b10052
J. Phys. Chem. B 2020, 124, 366−372

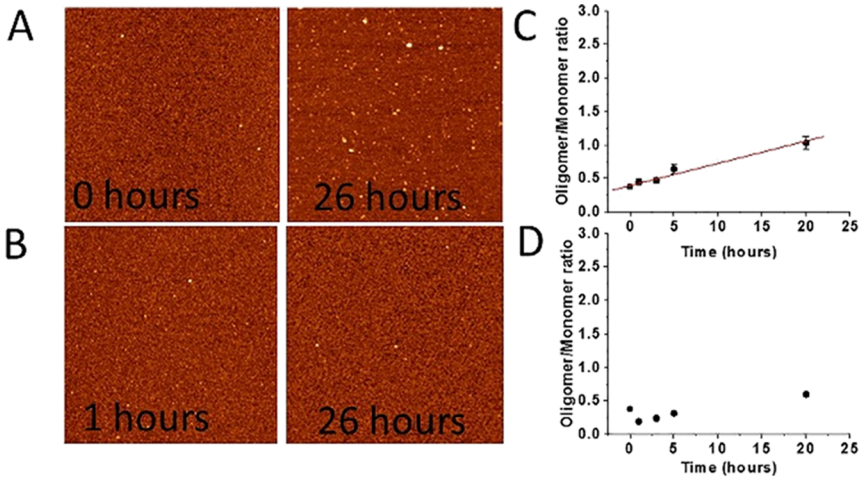

Figure 2. Experimental data for the aggregation of α-Syn. (A) AFM images of the on-surface aggregation of 2 nM α-Syn for 0 and 26 h. (B) AFM images of aggregation for 2 nM α-Syn in the bulk solution for 1 and 26 h. Scan sizes are 800 nm. (C) The time dependence of the oligomer-to-monomer ratio of 2 nM α-Syn in the on-surface aggregation and (D) in bulk solution.

$$\frac{dC_{oligo}(t)}{dt} = k_s C_1 C(t) \tag{9}$$

Here, we also assumed that C_1 is time-independent because the protein adsorption equilibrium is quickly established and the protein bulk concentration does not change quickly due to relatively slow reaction rates for the processes on the surface and much slower rates of bulk processes.

These equations can be easily solved to produce the following:

$$C(t) = C_0 e^{-k_s C_1 t} \tag{10}$$

$$C_{oligo}(t) = C_0(1 - e^{-k_s C_1 t}) \tag{11}$$

If the reaction rate on the surface is assumed to be relatively slow and/or the time is relatively short, then eq 11 can be expanded to linear terms of time, yielding the following:

$$C_{oligo}(t) \approx C_0 k_s C_1 t \tag{12}$$

From this expression, the ratio of oligomers to monomers on the surface as a function of time can be given by the following:

$$\frac{C_{oligo}}{C_1} \approx C_0 k_s t \tag{13}$$

This result predicts that the ratio of oligomers to the monomers will grow linearly with time, and it will be proportional to the original concentration of the protein monomers in bulk solution. Importantly, our theoretical model considers all oligomers. The detailed description of the model is presented in the Supporting Information as Additional Considerations Including All Oligomers. The result of the theory predicts the linear growth of the oligomer-to-monomer ratio on the surface with time as it is seen from eq S24.

AFM Studies of the Surface-Mediated Protein Aggregation. To experimentally test these theoretical predictions, an approach developed by us recently[17] was applied, as shown schematically in Figure 1. A mica sheet was placed in a test tube (Figure 1A) containing the protein solution and incubated at room temperature for a finite time; afterward, to directly count the number of aggregates appearing on the surface, the mica was removed, rinsed with water, dried, and imaged using AFM (Figure 1B). Such experiments were performed at different incubation times. As a control, aliquots were taken from the same protein solution, but no mica strip was added (Figure 1C). The AFM image for the control is shown in Figure 1D.

Figure 2A shows the results of experiments with 2 nM α-Syn in the presence of mica, imaged between 0 and 26 h. The data show that, over time, more globular features appear on surfaces, and their sizes also increase upon incubation. Figure S1 provides more images at times ranging from 1 to 20 h. Control samples (Figure 2B and Figure S2) did not show an observable change in the number of aggregates. Figure 2C,D provides quantitative analysis of the AFM images; in this graph, the ratio of oligomers to monomers is plotted as a function of time. The initial part of the kinetics of aggregation (between 0 and 20 h) is fitted by a linear plot (Figure 2C), supporting the prediction of the theoretical model (eq S21). The data for control experiments are shown in Figure 2D and did not reveal aggregate assembly in bulk solution.

Similar experiments were performed using an increased concentration of α-Syn (10 nM). AFM images of the on-surface aggregation process, taken at different times during incubation, are shown in Figure S3. These images clearly show that aggregates appear upon incubation, and their number and sizes increase over time. Control experiments obtained for the same incubation times (Figure S4) do not show such time-dependent α-Syn aggregation in bulk solution. Quantitative analyses of these data for on-surface aggregation and in bulk solution are presented in Figure S5A,B, respectively.

Similar to the data obtained for 2 nM α-Syn, the ratio of the number of oligomers to monomers increases gradually over time. The early aggregation kinetic graphs were fitted with the linear plot (Figure S5A), and the slope for 10 nM α-Syn turned out to be larger than that for 2 nM α-Syn, which is in line with the theoretical predictions. Meanwhile, no time-dependent aggregation was observed for 10 nM α-Syn in the bulk solution (Figure S5B), similar to control experiments for 2 nM α-Syn.

To further test theoretical predictions, experiments were performed with the A3G protein, which has a strong propensity toward oligomerization depending on its concentration in solution.[20] This feature is considered an additional mechanism for the antiviral activity of A3G. Figure 3A,B shows

https://dx.doi.org/10.1021/acs.jpcb.9b10052
J. Phys. Chem. B 2020, 124, 366−372

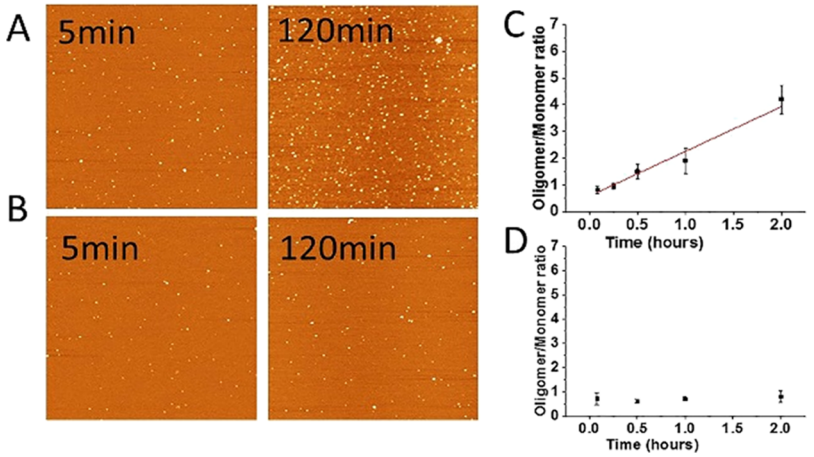

Figure 3. Experimental data for A3G protein aggregation. (A) AFM images of the on-surface aggregation of 1 nM A3G at 5 and 120 min. (B) AFM images of aggregation of 1 nM A3G in bulk solution at 5 and 120 min. Scan sizes are 1.5 microns. (C) The time dependence of the oligomer-to-monomer ratio of 1 nM A3G in the on-surface aggregation and (D) in the bulk solution.

AFM images of the on-surface aggregation of A3G at a concentration of 1 nM; the figures correspond to 5 and 120 min on-surface aggregation and in the bulk solution, respectively. Figure S6A,B provides additional AFM images at intermediate time intervals for the aggregation of A3G in the presence of the mica surface and in bulk solution, respectively. These images clearly show the accumulation of on-surface aggregates. No aggregation is observed for control experiments in bulk solution performed in parallel. Figure 3C shows a quantitative analysis of the initial process of the aggregation kinetics (between 0 and 2 h) fitted with a linear plot. On the other hand, aggregation of A3G in solution is not time-dependent, showing no change in the oligomer-to-monomer ratio over time (Figure 3D). Note that the number of monomers remains unchanged (Figure S7).

The quantitative data for 2 nM A3G for on-surface aggregation (A) and in bulk solution (B) are presented in Figure S8. The linear approximation for on-surface aggregation shows faster a aggregation process for 2 nM A3G than for 1 nM A3G. Table 1 assembles data characterizing the kinetics for the on-surface aggregation of both α-Syn and A3G proteins.

Table 1. Characterization of the Kinetics of On-Surface Aggregation for α-Syn and A3G Proteins

protein	concentration	C_0k_s (slope)
α-synuclein	2 nM	0.033
α-synuclein	10 nM	0.069
A3G	1 nM	1.672
A3G	2 nM	2.306

To demonstrate that on-surface aggregation does not depend on the type of surface, we performed similar experiments with the bare mica surface. The results for on-surface aggregation and in bulk solution for 1 nM A3G on bare mica are shown in Figure S9. Panels (A) and (B) are AFM images, which illustrate the on-surface aggregation of A3G over time compared to AFM images in panels (C) and (D), which demonstrate no aggregation in bulk solution. The analysis of the data as the dependence of the oligomer-to-monomer ratio on time with the linear fit of the early kinetic process is shown in the plot (panel (E)). No aggregation was observed in solution, as demonstrated in panel (F). These data together with the results in Figure 3 demonstrate that the accelerated aggregation does not depend on the surface type.

At the same time, according to the theory, the surface should not induce aggregation for non-aggregated protein. To confirm this, we performed experiments for on-surface aggregation for the PriA protein, which exists in solution as a monomer.[27,28] The data for on-surface aggregation experiments of 0.5 nM PriA are shown in Figure S10. The volume of the protein, obtained from AFM images (panels (A) and (B)) does not change over time as shown in panels (C) and (D), which indicates that PriA does not aggregate in the presence of the surface and remains in its monomeric state.

According to the theory (eq 2), the kinetics of on-surface aggregation depends on the affinity of the protein to the surface. The elevated propensity of A3G compared with α-Syn to form aggregates on the surface points to its high affinity for the mica surface; this feature is in line with the high affinity of this protein to the cellular membrane and other intracellular particles.[29,30]

Although the experimental results support the theoretical prediction regarding the linear dependence for the initial aggregation process on time (eq 13), the dependence on the concentration is not fully in line with theoretical predictions. According to Table 1, the 5-fold increase in the α-Syn concentration does not change the aggregation rate 5-fold; only a 2-fold increase is observed. However, this result is not surprising considering that the theory does not include factors such as changes in the protein conformation upon the interaction with surfaces. Moreover, the formation of oligomers larger than dimers also can influence aggregation kinetics. Indeed, our computational simulation previously showed that amyloid β-peptide (Aβ)[14−23] undergoes a conformational change that facilitates the assembly of dimers.[17] Based on our recent studies for the aggregation of α-Syn aggregation on membrane surfaces,[31] it is reasonable to assume that α-Syn also undergoes a conformational change at the mica−liquid interface. Meanwhile, comparison of α-Syn aggregation on membrane bilayers of different compositions induced different conformational changes and resulted in only several-fold changes in the aggregation propensities of membranes.[31] This value is considerably less than the overall aggregation catalysis of membranes and mica, which is in the range of several orders of magnitude;[17] such an acceleration is

https://dx.doi.org/10.1021/acs.jpcb.9b10052
J. Phys. Chem. B 2020, 124, 366−372

in line with the current theoretical predictions. However, understanding the effect of the membrane composition on the entire on-surface aggregation process can explain the role of membrane surfaces in the assembly of amyloid aggregates[31] and will help elucidate the molecular mechanisms behind protein-aggregation diseases such as Alzheimer's and Parkinson's diseases. The development of such a more comprehensive model is our long-term goal.

CONCLUSIONS

The data obtained support the physical−chemical model for which the key factor defining the on-surface aggregation process is transient binding of monomers that play the role as nuclei in the assembly of aggregates. Importantly, the model works not only for α-Syn, a typical member of amyloidogenic proteins capable of assembly into fibrils, as supported by numerous studies including ours,[32−34] but also for the A3G enzyme, for which the stoichiometry of aggregates is defined by the concentration of monomers.[20] Notably, unlike the amyloid aggregates that dramatically change the physiological function of monomers (ref 35 and the references therein), the assembly of A3G into oligomers contributes to the anti-HIV activity of A3G (ref 36 and the references therein).

ASSOCIATED CONTENT

Supporting Information

The Supporting Information is available free of charge at https://pubs.acs.org/doi/10.1021/acs.jpcb.9b10052.

Detailed description of the model; AFM images of on-surface and bulk aggregation of 2 and 10 nM α-Syn; plot of oligomer/monomer ratios for on-surface and bulk aggregation of α-synuclein; AFM images of on-surface and bulk aggregation of A3G; plot of oligomer/monomer ratios for on-surface and bulk aggregation of A3G; on-surface experiments of the non-aggregating PriA protein; volume analysis of monomeric A3G and α-Syn (PDF)

AUTHOR INFORMATION

Corresponding Authors

Anatoly B. Kolomeisky − *Rice University, Houston, Unites States;* orcid.org/0000-0001-5677-6690; Email: tolya@rice.edu

Yuri L. Lyubchenko − *University of Nebraska Medical Center, Omaha, Nebraska*; Email: ylyubchenko@unmc.edu

Other Authors

Yangang Pan − *University of Nebraska Medical Center, Omaha, Nebraska*

Siddhartha Banerjee − *University of Nebraska Medical Center, Omaha, Nebraska*

Karen Zagorski − *University of Nebraska Medical Center, Omaha, Nebraska*

Luda S. Shlyakhtenko − *University of Nebraska Medical Center, Omaha, Nebraska*

Complete contact information is available at: https://pubs.acs.org/10.1021/acs.jpcb.9b10052

Author Contributions

Y.L.L. and A.B.K. designed the project. Y.P., S.B., K.Z., and L.S.S. performed the AFM experiments and data analysis. A.B.K. provided the theoretical model. All authors contributed to writing the manuscript.

Notes

The authors declare no competing financial interest.

ACKNOWLEDGMENTS

This work was supported by grants to Y.L.L. from NIH (R01-GM118006, GM096039, and R21NS101504). A.B.K. was supported by the Welch Foundation (C-1559), the NSF (CHE-1664218), and the Center of Theoretical Biological Physics, sponsored by the NSF (PHY-1427654). We thank Dr. R. Harris and Dr. C. Rochet for providing the A3G and α-Syn proteins, respectively, and Dr. Lyubchenko's lab members for their fruitful discussions. We thank Melody A. Montgomery for editing this manuscript.

REFERENCES

(1) Hendrickson, W. A.; Pähler, A.; Smith, J. L.; Satow, Y.; Merritt, E. A.; Phizackerley, R. P. Crystal structure of core streptavidin determined from multiwavelength anomalous diffraction of synchrotron radiation. *Proc. Natl. Acad. Sci. U. S. A.* **1989**, *86*, 2190−2194.

(2) Tamulaitis, G.; Rutkauskas, M.; Zaremba, M.; Grazulis, S.; Tamulaitiene, G.; Siksnys, V. Functional significance of protein assemblies predicted by the crystal structure of the restriction endonuclease BsaWI. *Nucleic Acids Res.* **2015**, *43*, 8100−8110.

(3) Hardy, J.; De Strooper, B. Alzheimer's disease: where next for anti-amyloid therapies? *Brain* **2017**, *140*, 853−855.

(4) Gray, J. J. The interaction of proteins with solid surfaces. *Curr. Opin. Struct. Biol.* **2004**, *14*, 110−115.

(5) Kurnik, M.; Ortega, G.; Dauphin-Ducharme, P.; Li, H.; Caceres, A.; Plaxco, K. W. Quantitative measurements of protein-surface interaction thermodynamics. *Proc. Natl. Acad. Sci. U. S. A.* **2018**, *115*, 8352−8357.

(6) Andreasen, M.; Lorenzen, N.; Otzen, D. Interactions between misfolded protein oligomers and membranes: A central topic in neurodegenerative diseases? *Biochim. Biophys. Acta* **2015**, *1848*, 1897−1907.

(7) Lindberg, D. J.; Wesén, E.; Björkeroth, J.; Rocha, S.; Esbjörner, E. K. Lipid membranes catalyse the fibril formation of the amyloid-β (1−42) peptide through lipid-fibril interactions that reinforce secondary pathways. *Biochim. Biophys. Acta, Biomembr.* **2017**, *1859*, 1921−1929.

(8) Williams, T. L.; Serpell, L. C. Membrane and surface interactions of Alzheimer's Aβ peptide-insights into the mechanism of cytotoxicity. *FEBS J.* **2011**, *278*, 3905−3917.

(9) Canale, C.; Oropesa-Nuñez, R.; Diaspro, A.; Dante, S. Amyloid and membrane complexity: The toxic interplay revealed by AFM. *Semin. Cell Dev. Biol* **2018**, *73*, 82−94.

(10) Bucciantini, M.; Rigacci, S.; Stefani, M. Amyloid aggregation: Role of biological membranes and the aggregate-membrane system. *J. Phys. Chem. Lett.* **2014**, *5*, 517−527.

(11) Roher, A. E.; Kokjohn, T. A.; Clarke, S. G.; Sierks, M. R.; Maarouf, C. L.; Serrano, G. E.; Sabbagh, M. S.; Beach, T. G. APP/Aβ structural diversity and Alzheimer's disease pathogenesis. *Neurochem. Int.* **2017**, *110*, 1−13.

(12) Cheng, B.; Li, Y.; Ma, L.; Wang, Z.; Petersen, R. B.; Zheng, L.; Chen, Y.; Huang, K. Interaction between amyloidogenic proteins and biomembranes in protein misfolding diseases: mechanisms, contributors, and therapy. *Biochim. Biophys. Acta* **2018**, *1860*, 1876−1888.

(13) Rabe, M.; Soragni, A.; Reynolds, N. P.; Verdes, D.; Liverani, E.; Riek, R.; Seeger, S. On-surface aggregation of α-synuclein at nanomolar concentrations results in two distinct growth mechanisms. *ACS Chem. Neurosci.* **2013**, *4*, 408−417.

(14) Lin, Y.-C.; Li, C.; Fakhraai, Z. Kinetics of surface-mediated fibrillization of amyloid-β (12-28) peptides. *Langmuir* **2018**, *34*, 4665−4672.
(15) Lin, Y.-C.; Petersson, E. J.; Fakhraai, Z. Surface effects mediate self-assembly of amyloid-β peptides. *ACS Nano* **2014**, *8*, 10178−10186.
(16) Lucas, M. J.; Keitz, B. K. Influence of zeolites on amyloid-β aggregation. *Langmuir* **2018**, *34*, 9789−9797.
(17) Banerjee, S.; Hashemi, M.; Lv, Z.; Maity, S.; Rochet, J.-C.; Lyubchenko, Y. L. A novel pathway for amyloids self-assembly in aggregates at nanomolar concentration mediated by the interaction with surfaces. *Sci. Rep.* **2017**, *7*, 45592.
(18) Proctor, E. A.; Fee, L.; Tao, Y.; Redler, R. L.; Fay, J. M.; Zhang, Y.; Lv, Z.; Mercer, I. P.; Deshmukh, M.; Lyubchenko, Y. L.; et al. Nonnative SOD1 trimer is toxic to motor neurons in a model of amyotrophic lateral sclerosis. *Proc. Natl. Acad. Sci. U. S. A.* **2016**, *113*, 614−619.
(19) Banerjee, S.; Sun, Z.; Hayden, E. Y.; Teplow, D. B.; Lyubchenko, Y. L. Nanoscale Dynamics of amyloid β-42 oligomers as revealed by high-speed atomic force microscopy. *ACS Nano* **2017**, *11*, 12202−12209.
(20) Shlyakhtenko, L. S.; Lushnikov, A. Y.; Miyagi, A.; Li, M.; Harris, R. S.; Lyubchenko, Y. L. Atomic force microscopy studies of APOBEC3G oligomerization and dynamics. *J. Struct. Biol.* **2013**, *184*, 217−225.
(21) Lv, Z.; Krasnoslobodtsev, A. V.; Zhang, Y.; Ysselstein, D.; Rochet, J. C.; Blanchard, S. C.; Lyubchenko, Y. L. Direct detection of α-synuclein dimerization dynamics: single-molecule fluorescence analysis. *Biophys. J.* **2015**, *108*, 2038−2047.
(22) Lyubchenko, Y. L.; Shlyakhtenko, L. S.; Gall, A. A. Atomic force microscopy imaging and probing of DNA, proteins, and protein DNA complexes: silatrane surface chemistry. *DNA-Protein Interactions*; Humana Press, 2009, *543*, 337−351.
(23) Shlyakhtenko, L. S.; Gall, A. A.; Lyubchenko, Y. L. Mica functionalization for imaging of DNA and protein-DNA complexes with atomic force microscopy. *Cell Imaging Techniques*; Humana Press, 2013, *931*, 295−312.
(24) Lyubchenko, Y. L.; Gall, A. A.; Shlyakhtenko, L. S. Visualization of DNA and protein-DNA complexes with atomic force microscopy. *Methods Mol. Biol.* **2014**, *1117*, 367−384.
(25) Shlyakhtenko, L. S.; Gilmore, J.; Portillo, A.; Tamulaitis, G.; Siksnys, V.; Lyubchenko, Y. L. Direct visualization of the EcoRII−DNA triple synaptic complex by atomic force microscopy. *Biochemistry* **2007**, *46*, 11128−11136.
(26) Shlyakhtenko, L. S.; Lushnikov, A. Y.; Miyagi, A.; Li, M.; Harris, R. S.; Lyubchenko, Y. L. Nanoscale structure and dynamics of ABOBEC3G complexes with single-stranded DNA. *Biochemistry* **2012**, *51*, 6432−6440.
(27) Jezewska, M. J.; Bujalowski. Interactions of Escherichia coli replicative helicase PriA protein with single-stranded DNA. *Biochemistry* **2000**, *39*, 10454−10467.
(28) Bhattacharyya, B.; George, N. P.; Thurmes, T. M.; Zhou, R.; Jani, N.; Wessel, S. R.; Sandler, S. J.; Ha, T.; Keck, J. L. Structural mechanisms of PriA-mediated DNA replication restart. *Proc. Natl. Acad. Sci. U. S. A.* **2014**, *111*, 1373−1378.
(29) Moris, A.; Murray, S.; Cardinaud, S. AID and APOBECs span the gap between innate and adaptive immunity. *Front. Microbiol.* **2014**, *5*, 534.
(30) Posch, W.; Steger, M.; Knackmuss, U.; Blatzer, M.; Baldauf, H.-M.; Doppler, W.; White, T. E.; Hörtnagl, P.; Diaz-Griffero, F.; Lass-Flörl, C.; et al. Complement-opsonized HIV-1 overcomes restriction in dendritic cells. *PLoS Pathog.* **2015**, *11*, No. e1005005.
(31) Lv, Z.; Hashemi, M.; Banerjee, S.; Zagorski, K.; Rochet, J.-C.; Lyubchenko, Y. L. Assembly of α-synuclein aggregates on phospholipid bilayers. *Biochim. Biophys. Acta, Proteins Proteomics* **2019**, *1867*, 802−812.
(32) McAllister, C.; Karymov, M. A.; Kawano, Y.; Lushnikov, A. Y.; Mikheikin, A.; Uversky, V. N.; Lyubchenko, Y. L. Protein interactions and misfolding analyzed by AFM force spectroscopy. *J. Mol. Biol.* **2005**, *354*, 1028−1042.
(33) Lyubchenko, Y. L.; Sherman, S.; Shlyakhtenko, L. S.; Uversky, V. N. Nanoimaging for protein misfolding and related diseases. *J. Cell. Biochem.* **2006**, *99*, 52−70.
(34) Yu, J.; Malkova, S.; Lyubchenko, Y. L. Alpha-Synuclein misfolding: single molecule AFM force spectroscopy study. *J. Mol. Biol.* **2008**, *384*, 992−1001.
(35) Copani, A. The underexplored question of β-amyloid monomers. *Eur. J. Pharmacol.* **2017**, *817*, 71−75.
(36) Shlyakhtenko, L. S.; Dutta, S.; Banga, J.; Li, M.; Harris, R. S.; Lyubchenko, Y. L. APOBEC3G interacts with ssDNA by two modes: AFM studies. *Sci. Rep.* **2015**, *5*, 15648.

https://dx.doi.org/10.1021/acs.jpcb.9b10052
J. Phys. Chem. B 2020, 124, 366−372